# Cellular Responses to the Metal-Binding Properties of Metformin

**Lisa Logie,[1] Jean Harthill,[1] Kashyap Patel,[2] Sandra Bacon,[1,3] D. Lee Hamilton,[1] Katherine Macrae,[4] Gordon McDougall,[3] Huan-Huan Wang,[5] Lin Xue,[5] Hua Jiang,[5] Kei Sakamoto,[2] Alan R. Prescott,[4] and Graham Rena[1]**

In recent decades, the antihyperglycemic biguanide metformin has been used extensively in the treatment of type 2 diabetes, despite continuing uncertainty over its direct target. In this article, using two independent approaches, we demonstrate that cellular actions of metformin are disrupted by interference with its metal-binding properties, which have been known for over a century but little studied by biologists. We demonstrate that copper sequestration opposes known actions of metformin not only on AMP-activated protein kinase (AMPK)-dependent signaling, but also on S6 protein phosphorylation. Biguanide/metal interactions are stabilized by extensive π-electron delocalization and by investigating analogs of metformin; we provide evidence that this intrinsic property enables biguanides to regulate AMPK, glucose production, gluconeogenic gene expression, mitochondrial respiration, and mitochondrial copper binding. In contrast, regulation of S6 phosphorylation is prevented only by direct modification of the metal-liganding groups of the biguanide structure, supporting recent data that AMPK and S6 phosphorylation are regulated independently by biguanides. Additional studies with pioglitazone suggest that mitochondrial copper is targeted by both of these clinically important drugs. Together, these results suggest that cellular effects of biguanides depend on their metal-binding properties. This link may illuminate a better understanding of the molecular mechanisms enabling antihyperglycemic drug action. ***Diabetes*** **61:1423–1433, 2012**

The antihyperglycemic properties of biguanides were first discovered in 1929 (1,2) and largely overlooked until they were systematically re-examined some 30 years later (3), but their mechanism of action remains enigmatic. In the last 12 years, it has become clear that treatment of cells with metformin reduces mitochondrial respiration by inhibiting complex I (4,5), thus inducing activation of AMP-activated protein kinase (AMPK)-sensitive signaling (6). More recent evidence suggests that there are also AMPK-independent cellular effects of this drug, including inhibition of S6 kinase-dependent signaling (7,8) and suppression of hepatic gluconeogenesis via energy deficit (9), both of which were previously proposed to be AMPK-dependent. The effects of metformin on gluconeogenesis are thought to account for much of the drug's antihyperglycemic properties and are still understood to depend on inhibition of mitochondrial respiration (4,9).

Recently, we have studied metal-dependent effects of small molecules on insulin signaling (10), leading us to become interested in the metal-binding properties of metformin itself. Compelling evidence of direct binding of metformin to metal ions, including extensive crystallographic (11) and spectroscopic analysis (12–14), contrasts with the paucity of evidence regarding direct binding of metformin to protein targets. Interaction of biguanides with metals has been known since the 19th century (15), just a few years after their synthesis and before their antihyperglycemic properties were first reported. Studies on this phenomenon have established not only that metformin acts as a ligand for a variety of divalent transition metals, but also that the most stable interactions by far are with copper (12,15–17) (Fig. 1*A*). More recently, copper has emerged as an important regulator of cardiac health with the potential to contribute toward the cardioprotective properties of metformin (18). This led us to use two independent approaches to interfere with metformin's copper-binding properties to study the impact on cellular responses to this drug. Moreover, we also exploited one of these approaches to study a second clinically important antidiabetic drug, pioglitazone. Our results suggest that the ability of these two widely used antihyperglycemic drugs to target copper ions contributes to their cellular actions.

## RESEARCH DESIGN AND METHODS

**Materials.** All chemicals were sourced commercially at the highest purity that we could obtain. The compounds were dissolved in Dulbecco's modified Eagle's medium (DMEM), except for pioglitazone, which was prepared in DMSO. The phospho-acetyl coenzyme A carboxylase (ACC) ($Ser^{79}$) and total vasodilator-stimulated phosphoprotein (VASP) antibody (S407B, first bleed) were a generous gift from the Division of Signal Transduction Therapy at the University of Dundee and the phospho-S6 ($Ser^{240/244}$), phospho-AMPK ($Thr^{172}$); total AMPK and β-actin antibodies for immunoblotting came from Cell Signaling Technology. Antibodies used for immunoprecipitation and assay of AMPK were a generous gift from Prof. D. Grahame Hardie's group.

**Cell culture and lysis for immunoblotting.** H4IIE liver cells (American Type Culture Collection) were chosen because they preserve glucocorticoid and insulin-sensitive regulation of hepatic gluconeogenic genes (19) and grown in DMEM plus 5% fetal calf serum for 20 passages. Two hours before stimulation, cells were placed in DMEM without serum, except for experiments involving 18-h triethylaminetetramine (trien) pretreatment, in which serum was removed at the same time as trien addition. Cells were lysed and prepared for SDS-PAGE essentially as described previously (20–22), using buffer A (50 mM Tris acetate [pH 7.5], 1% [volume for volume] Triton X-100, 1 mM ethylenediamine tetraacetic acid [EDTA], 1 mM ethylene glycol-bis[β-aminoethyl ether]-*N*,*N*,*N*′*N*′-tetraacetic acid [EGTA], 0.27 M sucrose, 50 mM NaF, 1 mM sodium orthovanadate, 10 mM β-glycerophosphate, 5 mM sodium pyrophosphate, 1 mM benzamidine, 0.2 mmol/L phenylmethylsulfonyl fluoride, and 0.1% [volume for volume] β-mercaptoethanol). Protein concentration was determined

From the [1]Division of Cardiovascular and Diabetes Medicine, Ninewells Hospital and Medical School, University of Dundee, Dundee, Scotland, U.K.; the [2]Medical Research Council Protein Phosphorylation Unit, College of Life Sciences, University of Dundee, Dundee, Scotland, U.K.; [3]The James Hutton Institute, Dundee, Scotland, U.K.; the [4]Division of Cell Signalling and Immunology, College of Life Sciences, University of Dundee, Dundee, Scotland, U.K.; and the [5]Beijing National Laboratory for Molecular Sciences, CAS Key Laboratory of Photochemistry, Institute of Chemistry, Chinese Academy of Sciences, Beijing, People's Republic of China.

Corresponding author: Graham Rena, g.rena@dundee.ac.uk.

Received 11 July 2011 and accepted 7 February 2012.

DOI: 10.2337/db11-0961

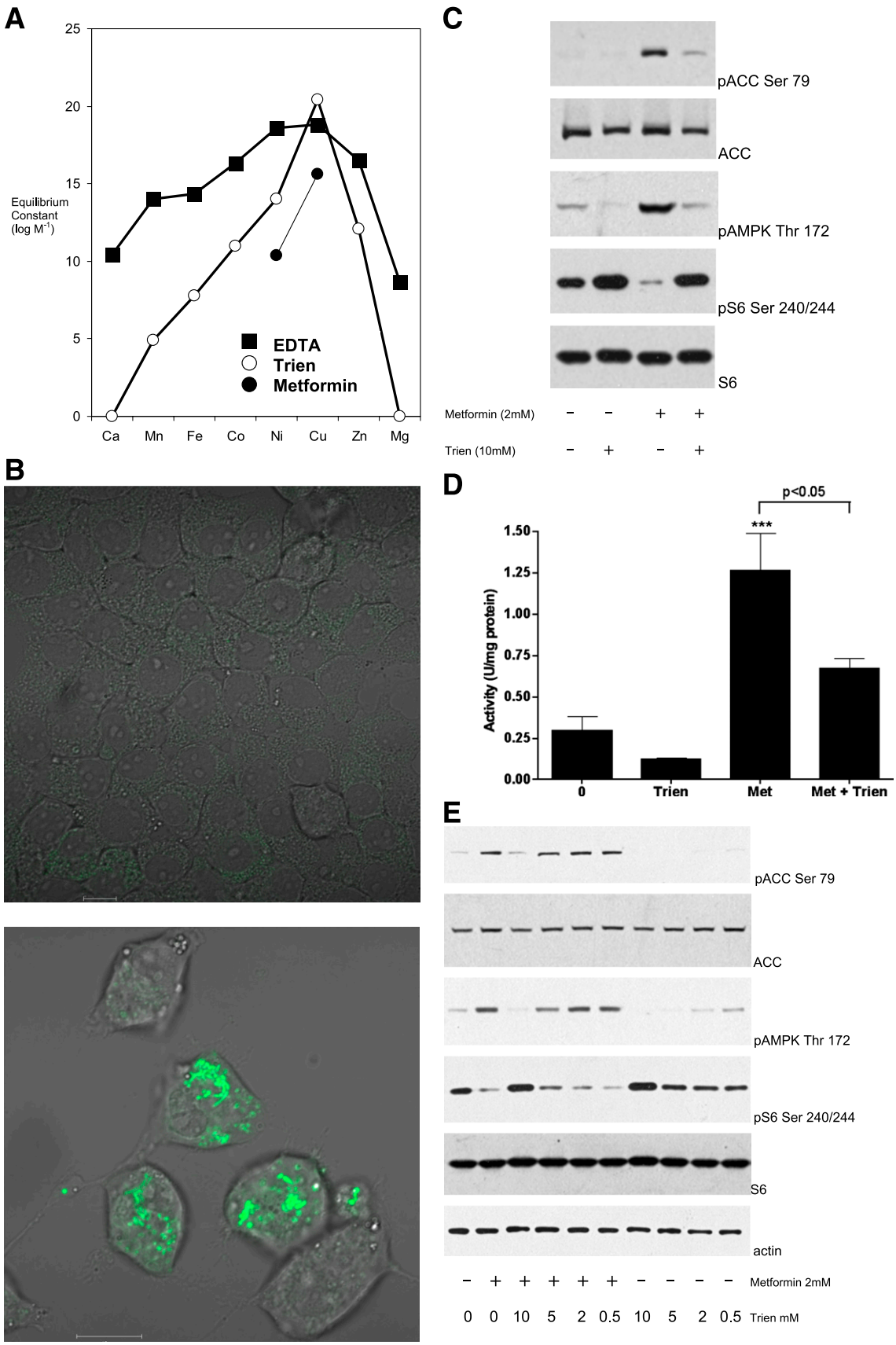


**FIG. 1. Trien opposes the action of metformin on AMPK and signaling to S6. *A*: Graph of the available stability constants for EDTA, triethylaminetetramine (trien), and the cumulative constant for a 2:1 dimethylbiguanide (metformin)/metal complex (data obtained from Refs. 17,25,26). Biguanides do not form stable complexes with zinc or alkaline earth metals (17). *B*: Cells placed in serum-free medium treated with (*bottom*)/without (*top*) 10 mM trien for 18 h were treated with the copper-binding probe followed by washout and image capture on the confocal microscope. Scale bar, 10 μm. *C*: Preincubation of cells with trien inhibits metformin's effects on AMPK Thr$^{172}$ phosphorylation (pAMPK), ACC Ser$^{79}$ phosphorylation (pACC),**

by Bradford assay (Pierce). Unless stated elsewhere, results are representative of at least three experiments.

**Preparation of cell extracts for kinase assays.** Cells were washed twice in ice-cold phosphate-buffered saline and scraped into ice-cold lysis buffer (50 mmol/L Tris-HCl [pH 7.4], 50 mmol/L sodium fluoride, 5 mmol/L sodium pyrophosphate, 1 mmol/L EDTA, 1 mmol/L EGTA, 150 mM sodium chloride, 1 mmol/L dithiothreitol [DTT], 0.1 mM benzamidine, 0.1 mM phenylmethylsulfonylfluoride, 1% Triton X-100, and 5 μg/mL soybean trypsin inhibitor). Cell debris was removed by centrifugation at 13,000 × *g* for 15 min at 4°C and protein concentration measured.

**Immunoprecipitation and assay of AMPK.** Cell extracts containing 33 μg protein were incubated overnight at 4°C on a shaking platform with protein G-sepharose conjugated to both anti-AMPKα1 and AMPKα2 antibodies (23). The immunocomplexes were pelleted and washed twice with 1 mL ice-cold buffer (50 mM Tris-HCl [pH 7.4], 50 mM NaF, 5 mmol/L sodium pyrophosphate, 1 mM EDTA, 1 mM EGTA, 1.15 M NaCl, 1 mM DTT, 1 mM benzamidine, 0.1 mM phenylmethylsulfonylfluoride, 1% Triton X-100, and 5 μg/mL soybean trypsin inhibitor) and once with ice-cold HEPES buffer (50 mM HEPES [pH 7.4], 0.03% Brij-35, and 1 mM DTT). AMPK activity was assayed at 30°C in the presence of 0.1 μCi of [γ-$^{32}$P]ATP, 0.33 mM cold ATP, 8.3 mM $MgCl_2$, 0.33 mM AMP, and 0.33 mM SAMS peptide (Division of Signal Transduction Therapy). Activity is expressed as the amount of AMPK catalyzing the phosphate incorporation of 1 nmol substrate in 1 min/mg of protein. Each bar of a graph consists of data from at least six separate immunoprecipitations, each one from a separate dish of cells.

**RNA isolation and real-time PCR.** Total RNA was extracted using TRIreagent (Sigma-Aldrich) and cDNA made using Superscript II reverse transcriptase (Invitrogen). Real-time PCR was done on an ABI Prism 7500 sequence detector (Applied Biosystems) using G6Pase primers (forward: 5′-CTCCAGCATGTACCGCAAAGA-3′, reverse: 5′-GGCTTCAGCGAGTCATGCAGA-3′) and probe (5′-AGTC GCTCCCATTCCGTTTGGCC-3′), incorporating 5′-6-carboxyfluorescein and 3′-6-carboxytetramethylrhodamine–fluorescent labels. 18S endogenous control was from Applied Biosystems. Cycling conditions were: 50°C for 2 min, 95°C for 10 min, followed by 40 cycles of 95°C for 15 s and 60°C for 1 min. Expression is expressed relative to 18s mRNA using the $2^{-\Delta\Delta Ct}$ method.

**Measurement of whole-cell oxygen consumption rate.** Using the Seahorse XF24 (Seahorse Bioscience), oxygen consumption rate (OCR) was measured essentially as described previously (6). Briefly, cells were plated at a density of 1 × $10^6$ cells/well in serum-containing medium. Once attached, cells were washed once in serum-free DMEM and incubated overnight. For the assay, cells were incubated in Krebs buffer (111 mM NaCl, 4.7 mM KCl, 2 mM $Mg_2SO_4$ 0.7 $H_2O$, 1.2 mM $Na_2HPO_4$, 2.5 mM glucose, and 0.5 mM carnitine). It was not possible to measure responses immediately after addition of drugs because it was necessary to adjust the pH of the buffer followed by degassing for 1 h. OCR was continuously measured for a period of 145 min. Cells were uncoupled by addition of 100 nM 2,4 dinitrophenol.

**Glucose production in primary hepatocytes.** Determination of hepatocyte glucose production was carried out essentially as described previously using primary mouse hepatocytes (9). Glucose production was determined after a 12-h incubation period in glucose-free DMEM with or without 100 μmol/L $Bt_2$-cAMP, 2 mM metformin, 5 mM biguanide, or 5 mM propanediimidamide. At the end of the incubation period of 12 h, medium was collected and mixed with 0.2 mL $HClO_4$ (40% volume for volume). After neutralization, glucose released into the medium was determined using glucose hexokinase reagent (Thermo Scientific) and then normalized to the total protein content per well.

**Determination of intracellular copper binding by fluorescence microscopy.** We used a novel copper probe, merocyanine dye-1 (DPD, Fig. 2) (24), that fluoresces in the absence of copper binding but, upon interaction with copper, the fluorescence is quenched. It has been shown that no other metal can substitute for copper to mediate this quenching, and, in competition studies, no other metal tested could compete to remove the copper (24), suggesting that DPD is a specific sensor of copper ions. H4IIE cells were incubated in 10 mM trien for 18 h or other compounds for 3 h at the doses indicated in the figure legends. After this incubation, 14 μM of DPD was added to all dishes with the exception of the no probe control. Cells were incubated in DPD for 30 min before washing once with serum-containing media to remove excess probe and compound (as described in Ref. 24). Cells were imaged immediately after washing using a Zeiss LSM700 confocal microscope (Carl Zeiss). Images were obtained using the 488-nm excitation laser, and the emissions were collected at 510–560 nm. Images were collected from fields of view visualized using differential interference contrast optics and then subsequent fluorescent imaging at original magnification ×100. The images shown in this study are representative of at least three separate random fields of view.

## RESULTS

**Copper sequestration inhibits induction of AMPK activity and dephosphorylation of S6.** To test the role of copper in metformin action, we first sought a high-affinity copper-binding compound that was more selective than metal-sequestering compounds commonly used in biology, such as EDTA. We chose trien (structure in Fig. 2) because it is highly selective for copper among the transition metals (25,26) (Fig. 1) and displays no binding activity toward biologically important alkaline earth metals such as calcium and magnesium (26). Owing to its hydrophilic nature, trien is thought not to enter cells, but depletes cellular copper by sequestration of extracellular copper (27). Together, these features have undoubtedly promoted trien's widespread clinical use to reverse copper overload in Wilson disease. To establish that trien can sequester intracellular copper, we used a cell-permeable copper-specific probe that fluoresces only in the absence of available copper (24). We found that in the absence of trien, fluorescence was observed in very few cells (Fig. 1*B*); however, following treatment of cells with 10 mM trien, we observed punctate cytoplasmic fluorescence in an increased number of cells, indicating that in these cells, there is insufficient copper available to quench the probe (Fig. 1*B*). Next, we tested whether preincubation with trien could block the signaling effects of metformin. Using H4IIE cells, we found that preincubation with trien opposed the actions of metformin on phosphorylation of AMPK in the activation loop ($Thr^{172}$) of α catalytic subunit, its target ACC, and S6 protein (Fig. 1*C*). Activation of AMPK signaling was further confirmed by performing a quantitative AMPK kinase assay after its immunoprecipitation from cell extracts (Fig. 1*D*). We found that trien pretreatment resulted in ~50% inhibition of metformin-induced AMPK activity (Fig. 1*D*). Trien also inhibited basal ACC and AMPK phosphorylation, consistent with the possibility that metformin acts to amplify an endogenous copper-dependent AMPK activation pathway. In dose-response experiments, we found that 5 mM trien incubation for 18 h was the minimum dose required to inhibit the action of 2 mM metformin (Fig. 1*E*).

**π-Electron delocalization intrinsic to biguanides is required for effects on AMPK but not S6.** We wished to obtain more direct evidence in support of a role for copper binding in the action of metformin in order to develop an understanding of what underlies the opposing effects of metformin and trien on signaling responses. These results can be rationalized if metformin but not trien acquires new properties when it binds copper. Previous work showed that metformin, which lacks aromatic character, and copper together form unusual pseudoaromatic planar ring structures, with square planar metal coordination replacing conventional tetragonal geometry, stabilized by bonds exhibiting considerable double-bond character due to extensive π-electron delocalization

**and S6 $Ser^{240/244}$ phosphorylation (pS6). H4IIE cells were grown in serum-free medium for 18 h in the presence or absence of 10 mM trien, followed by stimulation with or without 2 mM metformin. Lysates were prepared as described in RESEARCH DESIGN AND METHODS then subjected to SDS-PAGE, followed by immunoblotting with the antibodies indicated. *D*: Cells were treated as in *C*, except 1 mM metformin (Met) was used, before lysis, immunoprecipitation, and AMPK assay as described in RESEARCH DESIGN AND METHODS. Statistical significance was determined by one-way ANOVA followed by Tukey post hoc test, ***$P < 0.001$ with respect to control. The significance of other column-to-column differences are presented next to a horizontal line identifying the two columns. Errors are SEM. *E*: Cells were treated as in *C* but in the presence of a dose response of trien. (A high-quality digital representation of this figure is available in the online issue.)**

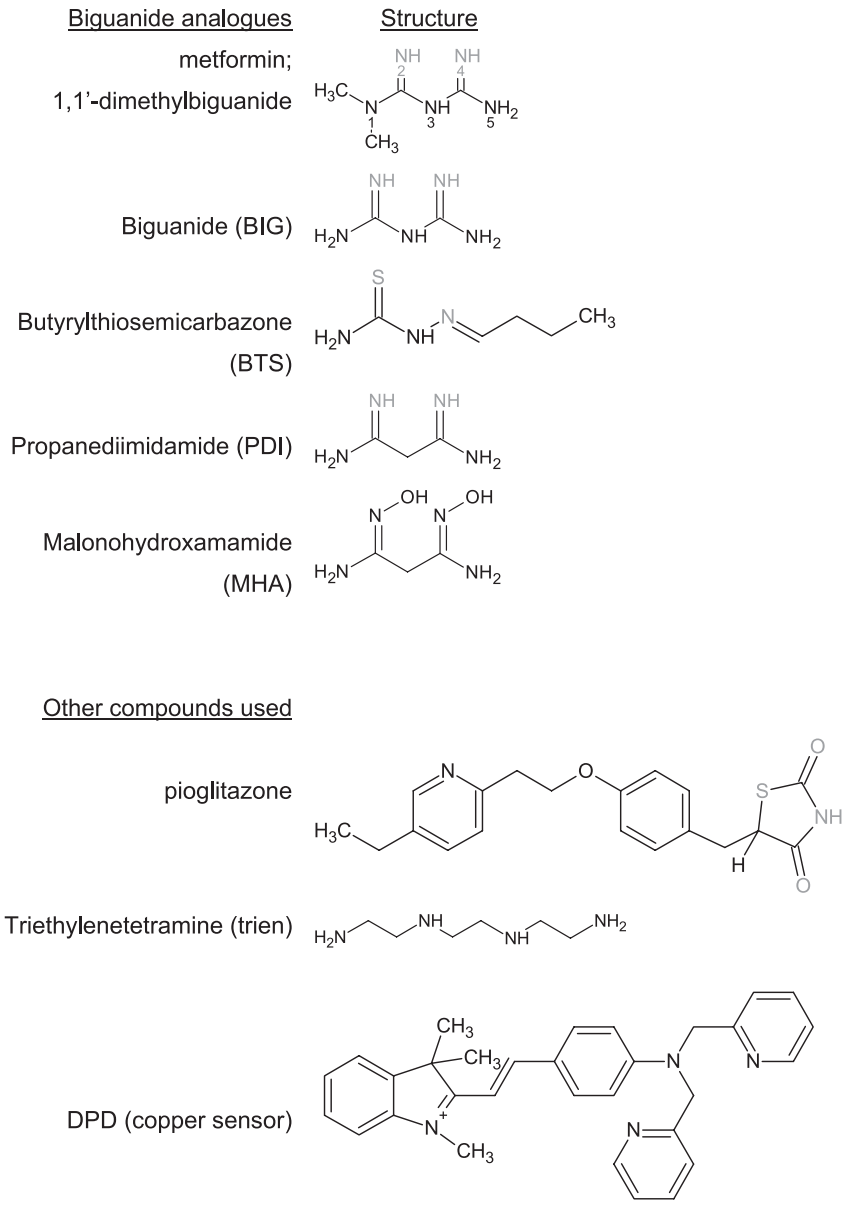


**FIG. 2. Compounds used in this study. Known metal coordinating ligands appear for each biguanide analog in gray. In pioglitazone, gray highlighting denotes the region of similarity between glitazones and metformin, along with the sulfur atom that undergoes oxidation-enabling linearization of the thiazolidinedione moiety. Chemical structures were drawn using ChemSketch (Advanced Chemistry Development, Inc.).**

(11,12). We noted that such a putative drug/target interaction unlocks novel chemical properties not only in the target copper (altered coordination geometry, Fig. 3*A*) but also in the drug metformin (aromaticity, Fig. 3*B* and *C*). Trien, in contrast, binds copper exclusively through single bonds, forming complexes that retain distorted axial liganding to the copper with no aromatic character (28). We reasoned that these differences in the character of interaction with copper might account for the differing effects on AMPK and S6 signaling of these two drugs.

To test the role of electron delocalization in the cellular action of biguanides, we studied a targeted panel of metformin derivatives in which, compared with metformin, π-electron ring delocalization is first weakened (compound butyrylthiosemicarbazone [BTS], Fig. 3*B*) and then abolished (compound propanediimidamide [PDI], Fig. 3*B*). Earlier studies indicated that diimidamides are not antihyperglycemic (29), suggesting that lack of efficacy could be mediated by the structural consequences of diminishing electron delocalization, which include formation of less stable, nonaromatic (12), and progressively less planar metal complexes (11,12,30–32). When we investigated ACC and AMPK phosphorylation in dose-response experiments, we found that it closely mirrored the extent of electron ring delocalization in each compound, as it was present in the two biguanides in the panel, metformin and biguanide (BIG), but reduced in BTS and absent in PDI (Fig. 3*B*). In contrast, S6 phosphorylation was inhibited similarly by metformin, BIG, BTS, and PDI. The differences in AMPK phosphorylation between BIG and PDI were also reflected in their ability to activate AMPK, as we found that BIG induced a twofold change in AMPK activity, but PDI did not activate AMPK (Fig. 3*D*). The fifth derivative that we studied was malonohydroxamamide (MHA). This compound is PDI that has been additionally modified so that the coordinating groups are blocked by hydroxylation (Fig. 2).

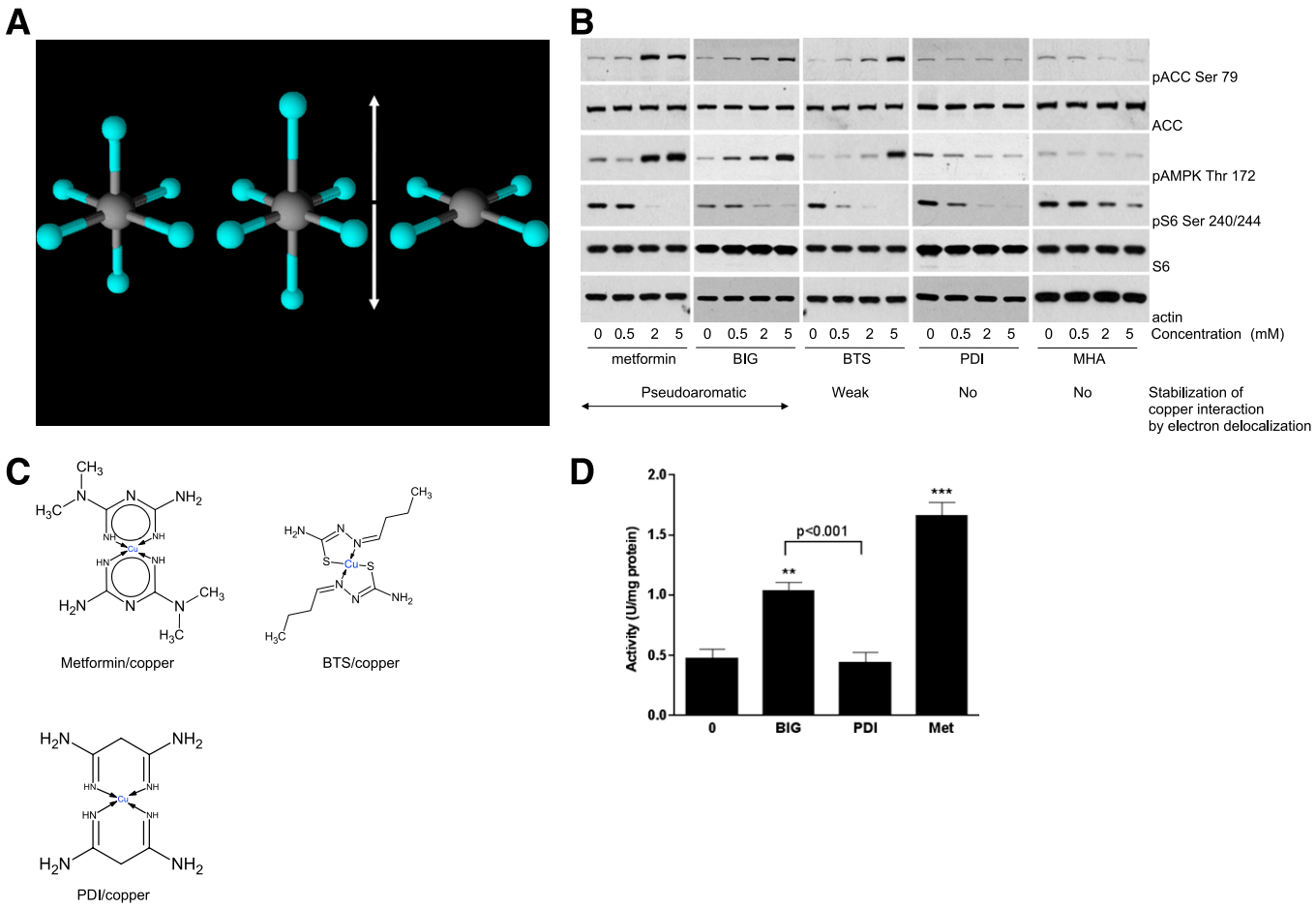


**FIG. 3. Interruption of π-electron delocalization intrinsic to biguanides results in compounds that selectively target S6 phosphorylation, lacking effects on AMPK. *A*: Commonly, distortion of copper $d^9$ octahedral coordination geometry (*left*) results in elongated axial ligands (*middle*). The extreme case of axial ligand elongation is the square planar structure (*right*). Copper is induced to adopt this geometry when metformin binds. *B* and *C*: H4IIE cells were grown in serum-free medium for 2 h, followed by stimulation with or without the metformin analogs shown, at the concentrations shown. Lysates were prepared for immunoblotting with the antibodies indicated. The chemical structures of metformin, BTS, and PDI complexed with divalent copper are shown in *C*. Metformin and BIG form pseudoaromatic planar complexes with copper in a square planar geometry, characterized by fairly uniform intermediate bond lengths in the ring, stabilized by π-electron delocalization (11–14). Thiosemicarbazones such as BTS also form extensively conjugated ring structures with copper (33); however, data on bond lengths (30,31), supported by spectroscopic studies (42), indicate that the resonance form shown predominates, with reduced delocalization of electron density and significant deviation from planarity compared with biguanides (11,14,31). PDI has π-electron delocalization in the ring abolished by substitution of N3 (12,32) and is not planar. *D*: H4IIE cells that had been deprived of serum for 2 h were treated with 2 mM of the agents shown for 3 h (metformin [Met]), before AMPK assay as described in RESEARCH DESIGN AND METHODS. Statistical analysis was carried out as in Fig. 1*D*. ***P* < 0.01, ****P* < 0.001. (A high-quality digital representation of this figure is available in the online issue.)**

In dose-response experiments with MHA, we found no effect on AMPK and inhibition of S6 phosphorylation was also very much reduced, with S6 phosphorylation readily detectable even at the highest concentrations of the drug (Fig. 3*B*). The results from this panel indicate that AMPK signaling is triggered only by derivatives capable of forming high-affinity pseudoaromatic planar structures with copper, whereas in contrast, S6 inhibition is supported unless the metal-liganding imine groups of the biguanide are blocked by direct modification.

**Effects of metformin analogs on mitochondrial respiration and hepatic glucose homeostasis.** Next, we examined nonsignaling responses to the metformin analogs. We found that PDI did not exhibit metformin-like inhibition of coupled mitochondrial OCR, nor could PDI replicate an additional effect of metformin in prolonging the duration of the maximal uncoupled mitochondrial OCR (Fig. 4*A*). We also studied effects of the compounds on gluconeogenic gene expression. Studying the metformin-regulated gluconeogenic gene glucose 6-phosphatase in H4IIE cells, we found that biguanides repressed expression of basal and cAMP-stimulated G6Pase (Fig. 4*B* and *C*), whereas PDI did not affect these responses. We were unable to detect significant effects of metformin on the expression of phosphoenolpyruvate carboxykinase (data not shown), consistent with earlier RT-PCR data using primary hepatocytes (9). When we investigated glucose production in primary hepatocytes, we found that biguanides suppressed hepatic glucose production but in contrast, PDI elicited a striking increase in glucose levels (Fig. 4*D*). This was not a result of increased cAMP levels, as judged by a VASP whole-protein antibody that exhibits a mobility shift (this faster migration is a result of phosphorylation of VASP) in response to increased intracellular cAMP levels (data not shown).

**Evidence that π-electron delocalization enables biguanides to compete for copper in cells.** Next, we wished to investigate how the π-electron delocalization intrinsic to metformin enables it to act. Most copper in biology is bound to proteins, and in this environment, many

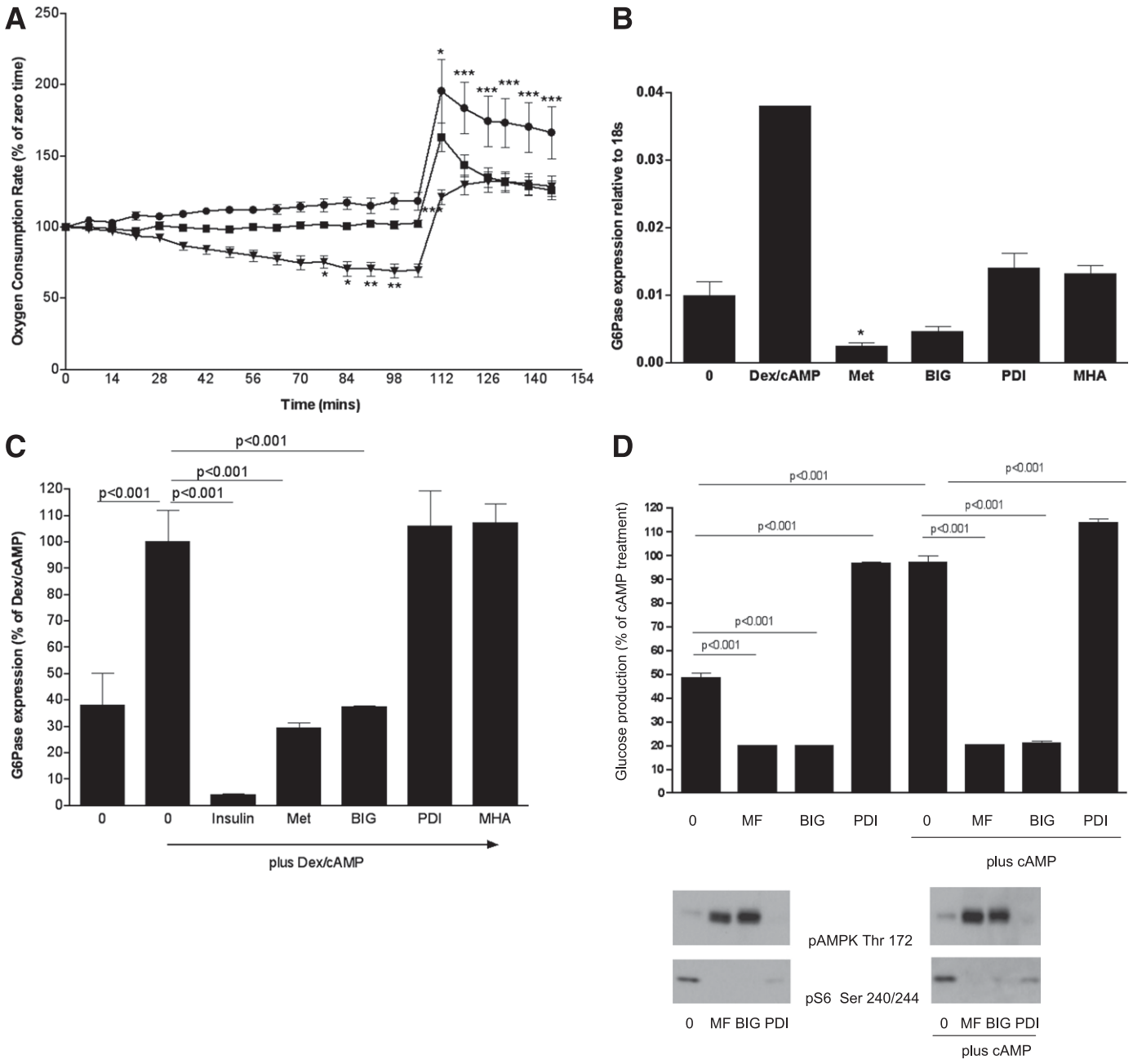


**FIG. 4. Effect of biguanides and PDI on mitochondrial respiration, gluconeogenesis, and glucose production. *A*: H4IIE cells were grown in serum-free medium overnight followed by stimulation without (squares) or with metformin (inverted triangles) or PDI (circles) as indicated. Cells were treated with drug 1 h before measurements started. Using a Seahorse analyzer (Seahorse Bioscience), OCR was measured. At 105 min, 100 μM 2,4 dinitrophenol was added to uncouple the electron transport chain from control by ATP synthesis in order to reveal the maximal respiration rate. There were no statistically significant differences in OCR between different treatment groups at time zero. Data are normalized to 100 at the start of the experiment. Statistical analysis was carried out as in Fig. 1*D*, except that a two-way ANOVA was performed. *B* and *C*: H4IIE cells were grown for 3 days, then serum-starved overnight, followed by stimulation for 8 h with or without 500 nM dexamethasone (Dex)/100 μM CPT-cAMP, coincubated with 10 nM insulin or the metformin analogs shown (2 mM of each, abbreviations are as in the main text). Expression of G6Pase was measured by RT-PCR, using conditions described in RESEARCH DESIGN AND METHODS. Statistical analysis was carried out as in Fig. 1*D*. *D*: Primary hepatocytes were treated with or without 2 mM metformin (MF), 5 mM BIG, or 5 mM PDI for 12 h with or without 100 μM $Bt_2$-cAMP and glucose production was measured as described in RESEARCH DESIGN AND METHODS. The cells were lysed and effects of the drugs on cell signaling verified by Western blotting (*bottom*). Statistical analysis was carried out as in Fig. 1*D*. *$P < 0.05$, **$P < 0.01$, ***$P < 0.001$.**

copper-binding drugs like trien, which provides four binding ligands for copper per molecule, probably displace copper simply by contributing more ligands than the competing protein (28,33). In contrast, metformin contains only two copper-binding ligands per molecule, which will not usually be sufficient to compete with most proteins for copper; however, we considered the possibility that the effects of π-electron delocalization on coordination geometry and double-bond character of the metformin/copper interaction might enable metformin to interact with copper in cells. To test this, we made use of the copper probe that we had used earlier in the study. We found that the biguanides increased punctate fluorescence of the copper probe, just as effectively as trien itself (Figs. 1*B* and 5*B*), but in contrast, PDI,

which lacks π-electron delocalization, and MHA, which lacks π-electron delocalization and free imine groups, were both unable to affect the fluorescence of the copper probe (Fig. 5*C*). Together, these observations provide evidence that the π-electron delocalization of biguanides not only promotes AMPK activation (Fig. 3) but also interaction with copper in cells (Fig. 5).

**Investigation of the role of copper in the action of another insulin-sensitizing drug, pioglitazone.** Next, we investigated the thiazolidinedione pioglitazone for similar effects to those that we had observed with metformin. Thiazolidinediones are generally understood to mediate most of their antidiabetic effects by acting as peroxisome proliferator–activated receptor γ agonists; however, more

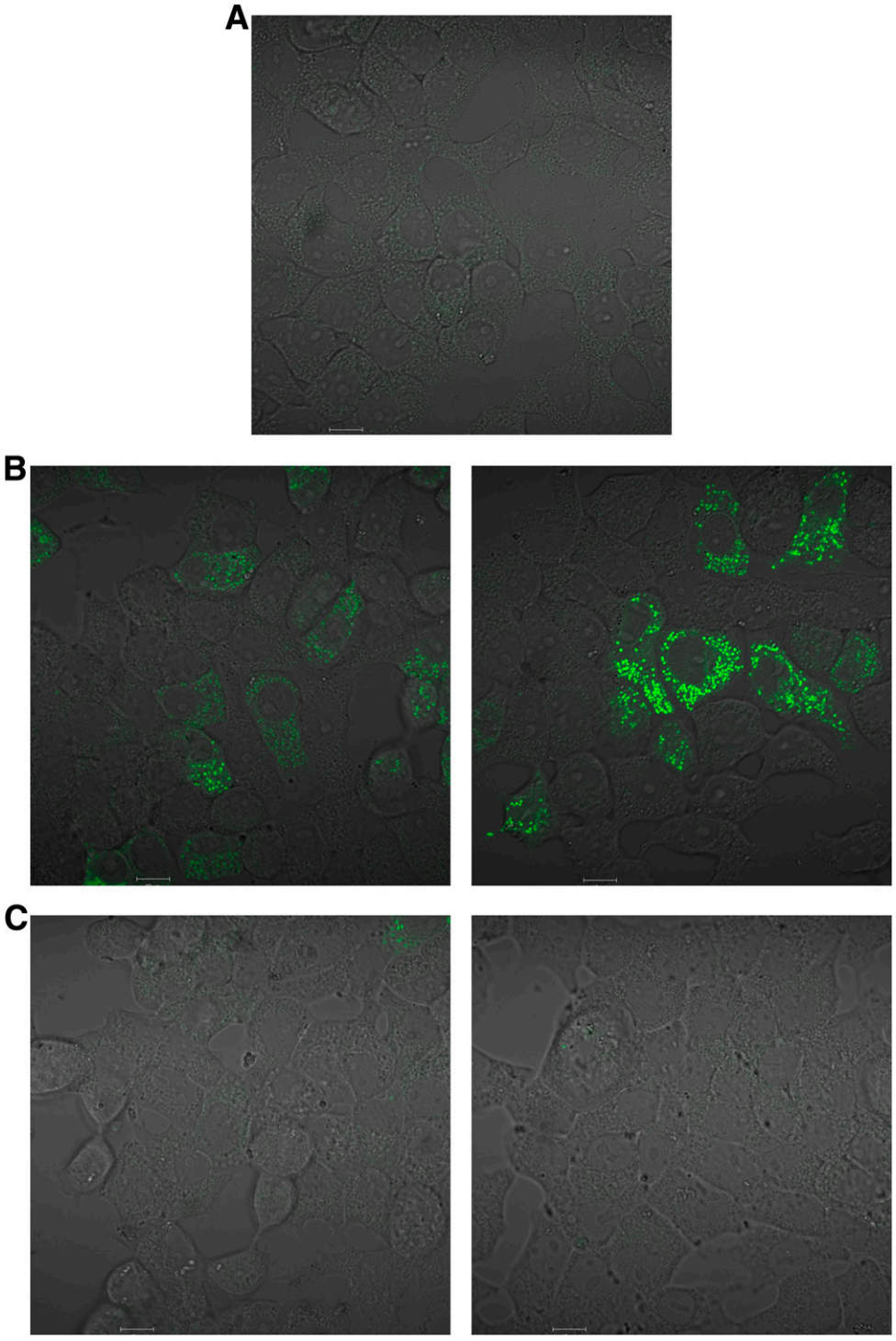


**FIG. 5. Effect of metformin analogs on the copper-specific fluorescent probe. Cells were serum-starved for 2 h before treatment for 3 h without (*A*) or with the biguanides metformin (*left*) and BIG (*right*) (*B*) or PDI (*left*) and MHA (*right*) (*C*). In each case, the cells were incubated in the presence of the copper-specific probe, before washout and visualization on the confocal microscope as discussed in RESEARCH DESIGN AND METHODS. Scale bars, 10 μm. (A high-quality digital representation of this figure is available in the online issue.)**

recent studies found that in addition they regulate AMPK signaling, activating this pathway with a half-maximal effective concentration ~20–40 times lower than metformin (34,35). In our experiments, we found that trien inhibited the effects of submaximal doses of pioglitazone on AMPK and S6 signaling (Fig. 6*A* and *B*). At higher concentrations of pioglitazone, we found that these effects of trien were abolished, demonstrating that these signaling pathways are not irreversibly desensitized by trien. We tentatively attribute pioglitazone's dominance to the greater hydrophobicity of this compound, which may allow it to accumulate in the cell much more readily than either trien or metformin. We have noticed that the thiazolidinedione ring moiety is structurally analogous to the metal-coordinating central N2–N4 portion of metformin, with a coordinating = O substituted for = NH. This part of the molecule becomes linearized in vivo by oxidation of the sulfur atom (36), substitution of which results in compounds with reduced antihyperglycemic efficacy (37); however, further work will be required to determine whether or not these structural similarities contribute toward the common effects of pioglitazone and biguanides that we have observed.

**Evidence that antihyperglycemic drugs regulate mitochondrial copper.** Exploiting the copper-sensitive probe again, we found that pioglitazone induced punctate fluorescence, suggesting that pioglitazone can affect copper in the cell like the biguanides (Fig. 7*A*). We wished to identify the localization of the punctate staining of the copper sensor that we had observed, and the first possibility that we considered was the mitochondria, as these have long been considered a likely locus of the actions of biguanides and thiazolidinediones (4,38,39), including triggering of effects on AMPK by inhibiting ATP production (6). To investigate this, we made use of a mitochondrial marker that fluoresces in the far red channel (excitation maximum 644 nm, emission maximum 665 nm). We found that the increased fluorescence of the copper probe in response to pioglitazone colocalized with this mitochondrial marker, suggesting that this drug reduces the amount of available copper in the mitochondria (Fig. 7*B*). We obtained similar results with metformin (Fig. 7*C*). These results suggest that targeting of mitochondrial copper is a common property of these two clinically relevant antihyperglycemic drugs.

## DISCUSSION

Increased hepatic glucose production is a major contributor to hyperglycemia in type 2 diabetes. Metformin is the leading treatment for improvement of glycemic control, with reduction of hepatic glucose output providing a major contribution to these effects. Even though it has been in widespread use for decades, the mechanisms underlying this action are not well-characterized. The most widely accepted current cellular model is that metformin acts as a mild, self-limiting (4) inhibitor of complex I in the mitochondria (4,5), leading in turn to AMPK-dependent (6) and AMPK-independent (7,9) cellular effects. AMPK-independent effects of metformin include suppression of hepatic gluconeogenesis (9), which is thought to occur in direct response to mitochondrial respiratory inhibition (4,9) and to account for the antihyperglycemic effects of the drug.

The identity of the molecular target mediating these cellular effects of metformin has proved harder to resolve, and this prompted us to become interested in the metal-binding properties of metformin, which have been very well substantiated by X-ray crystallography (11) and spectroscopic approaches (12–14). This led us to wonder whether targeting of copper, the ion that binds metformin with the highest affinity (17), might contribute to the actions of the drug. Using two separate approaches, we found that cellular

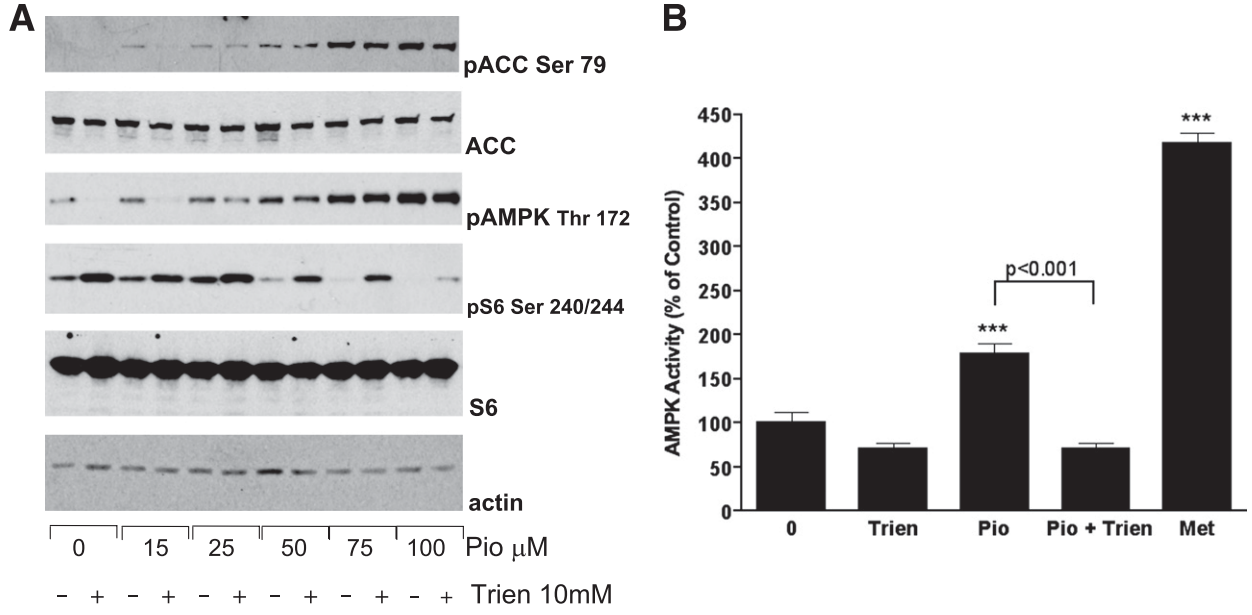


**FIG. 6. Effect of trien on cell signaling responses to pioglitazone. *A*: H4IIE cells were grown in serum-free medium for 18 h in the presence or absence of 10 mM trien, followed by stimulation with or without differing doses of pioglitazone, as indicated. Lysates were prepared for immunoblotting with the antibodies indicated as described in RESEARCH DESIGN AND METHODS. *B*: H4IIE cells were grown in serum-free medium for 18 h in the absence or presence of 10 mM trien. Individual dishes were then stimulated without or with 15 μM pioglitazone (Pio) for 3 h. Total of 2 mM metformin (Met) was added to further dishes for 3 h as a positive control, and then the samples were prepared for AMPK assay as described in RESEARCH DESIGN AND METHODS. Statistical analysis was carried out as in Fig. 1*D*. ***$P < 0.001$.**

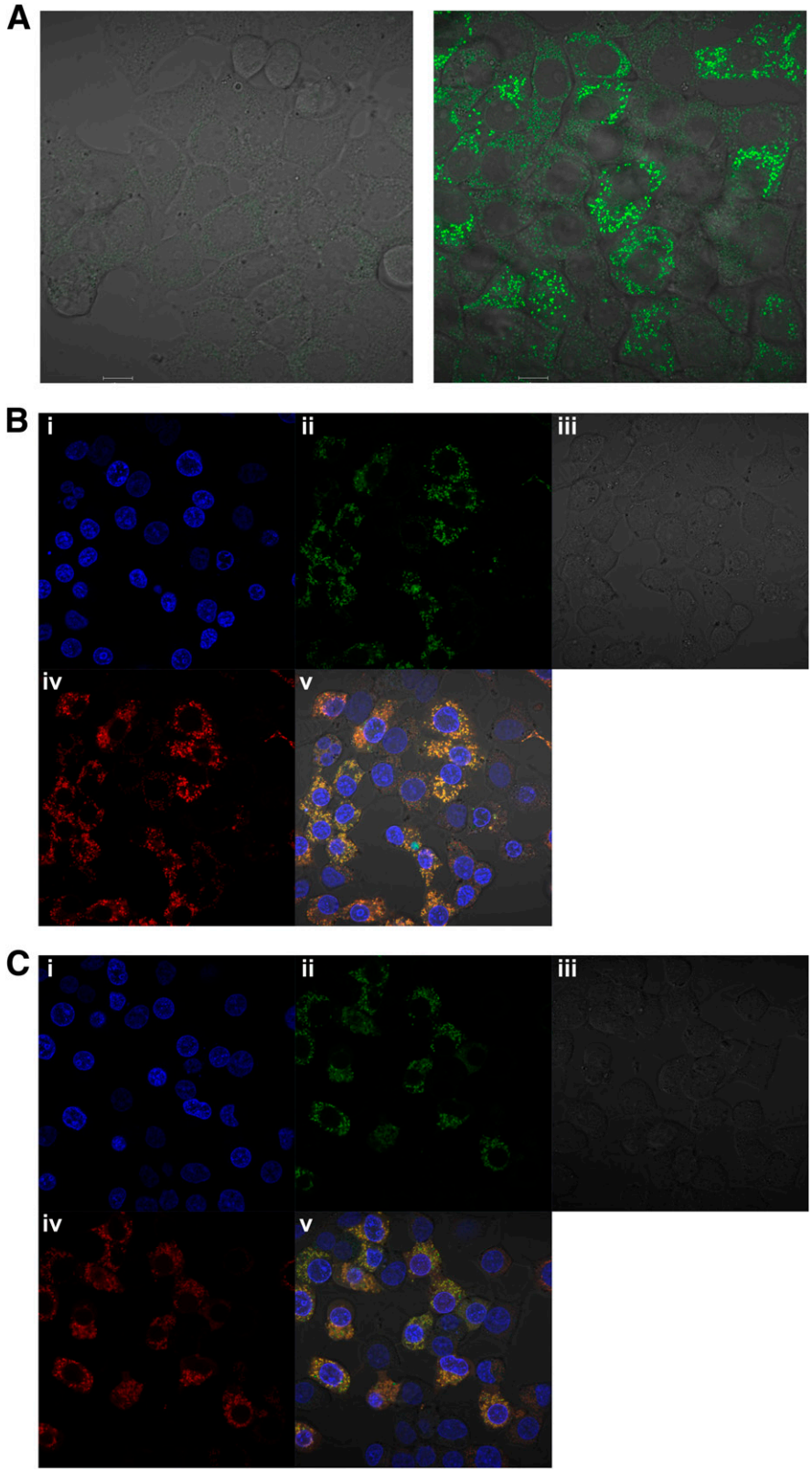


**FIG. 7. Evidence that metformin and pioglitazone regulate mitochondrial copper. *A*: H4IIE cells were grown in serum-free medium for 2 h before treatment with (*right*) or without (*left*) 100 μM pioglitazone for 3 h. In each case, the cells were incubated in the presence of the copper-specific probe, before washout and visualization on the confocal microscope as discussed in RESEARCH DESIGN AND METHODS. Scale bars, 10 μm. *B* and *C*: Cells were serum-starved for 2 h before treatment for 3 h with 100 μM pioglitazone (*B*) or 2 mM metformin (*C*). The cells were incubated in the presence of the copper-specific probe (green channel, *ii*) and a mitochondrial marker (far red channel, *iv*), before washout and visualization on the confocal microscope as discussed in RESEARCH DESIGN AND METHODS. Hoechst staining (blue channel, *i*) marks the nucleus. All channels are merged in *v* to demonstrate colocalization. *Panel iii* is phase-contrast. (A high-quality digital representation of this figure is available in the online issue.)**

responses of metformin are related to the drug's metal-binding properties. In the first approach, preincubation of cells with the copper-sequestering drug trien inhibited responses to metformin on its two key signaling outputs, the AMPK and S6 signaling pathways. We do not exclude the possibility that other biologically important metal ions could contribute to these effects, but our results support copper involvement for the following three reasons: firstly, copper is the ion that both metformin and trien bind with the highest affinity; secondly, we observed similar effects of both drugs on a cell-permeable copper-specific probe; and thirdly, metformin does not form stable interactions with zinc (17), which is the only other biologically abundant ion exhibiting appreciable affinity for trien.

These results led us to examine metformin analogs in which the affinity, geometry, and chemical properties of metal-binding are altered. Earlier studies indicated that structures similar to biguanides but lacking π-electron delocalization are not antihyperglycemic (29), suggesting that this property, which supports high-affinity pseudoaromatic planar copper interaction (12), is essential for the therapeutic properties of these drugs. Comparing the two signaling responses to biguanides, we found that effects on AMPK were much more sensitive to disruption of π-electron delocalization than were effects on S6 dephosphorylation. Thus, when we investigated analogs of metformin in which π-electron delocalization is weakened or absent, we found that AMPK responses were proportionately reduced and then abolished. In contrast, inhibition of S6 phosphorylation did not depend on π-electron delocalization at all, suggesting that inhibition of S6 may be insufficient by itself to endow antihyperglycemic properties. Inhibition of S6 phosphorylation was only affected by direct modification of the metal-liganding imine groups of the biguanide structure, suggestive of a lower-affinity copper interaction governing effects on this aspect.

The differing sensitivities of AMPK and S6 signaling to modification of the biguanide structure may suggest a dual action and/or separate thresholds controlling these two outputs and provide further pharmacological support for the proposal that the effects of biguanides on AMPK are not essential for effects on S6, as has been suggested recently by others (7,8). Additional studies with genetic mouse models indicate that AMPK itself is not sufficient for actions of metformin on hepatic glucose output and reducing blood glucose concentrations (9), suggesting that other mediators may be important. Our work with a fluorescent copper probe suggests that one potential mediator of metformin action, which we have demonstrated depends on π-electron delocalization of the drug, is targeting of mitochondrial copper, consistent with the known mitochondrial effects of the drug (4,5). We found that metformin but not its analog PDI inhibited basal mitochondrial respiration and caused a striking prolongation in the duration of the maximal respiration rate after uncoupling, suggesting that π-electron delocalization of metformin is required for both of these effects. Under the conditions we used, there was little nonmitochondrial respiration in these cells (data not shown), indicating that these are effects on mitochondrial respiration. In contrast, PDI tended to increase respiration, and after uncoupling, this became significant. At the doses we used, metformin did not noticeably reduce the initial slope of uncoupled respiration, in agreement with previous studies (6). This contrasts with responses in HEK293 cells, in which metformin does strongly inhibit uncoupled respiration (6), consistent with inhibition of the electron transport chain. Further work will be required to determine the reason for these cell-to-cell variations.

Studying gluconeogenic gene expression in H4IIE cells, a similar pattern emerged, as biguanides, but not PDI or MHA, were capable of inhibiting dexamethasone/cAMP-stimulated G6Pase expression and glucose production, suggesting that π-electron delocalization of biguanides is also required for these responses. When we investigated glucose production in primary hepatocytes, we found that biguanides suppressed this, but in unstimulated cells, PDI induced glucose production to a similar degree to cAMP, reminiscent of hyperglycemic characteristics exhibited by other guanidine analogs (40). PDI appears to do this in a cAMP-independent manner, suggesting that these two agents act on glucose production by different mechanisms, and we are currently investigating this. Taken together with the effects of metformin, the results with PDI are consistent with earlier evidence that changes in respiration trigger equivalent responses in glucose production (9,41). In addition to possible flux control effects, we and others (9) have observed accompanying changes in gluconeogenic gene expression and cellular signaling. Compared with S6, AMPK is the more reliable signaling marker of repression of glucose production and G6Pase expression, even though AMPK itself is dispensable for metformin's effects on these processes (9).

In summary, this study indicates that effects of metformin and related compounds on cell responses depend on their ability to interact with copper. It will be interesting therefore to investigate other compounds capable of forming stable pseudoaromatic planar complexes with copper, like metformin does, for antihyperglycemic, cardioprotective, and further potential therapeutic properties exhibited by metformin. More broadly, our results suggest that the number of targets for drug discovery could be widened not only by investigating nonprotein targets such as copper, but also by considering the role of metal-induced effects on chemical bonding and conformational geometries of drug structures.

## ACKNOWLEDGMENTS

This study was supported by Diabetes UK, The Rank Prize Funds, and Tenovus Scotland (to G.R.) and National Basic Research Program of China Grant 2011CB935800 (to H.J.). K.S. is supported by the United Kingdom Medical Research Council. K.P. is supported by the Wellcome Trust PhD Programme for Clinicians.

No potential conflicts of interest relevant to this article were reported.

L.L. performed almost all of the experiments presented with assistance from J.H., K.P., S.B., K.M., G.M., A.R.P., and G.R. D.L.H. carried out some preliminary experiments and showed L.L. how to do AMPK activity assays. H.-H.W., L.X., and H.J. synthesized and provided information on the copper sensor. G.R. designed most of the experiments, always in discussion with those actually carrying them out. L.L., A.R.P., and G.R. designed the microscopy experiments together, which were carried out in A.R.P.'s laboratory. K.P. and K.S. designed and carried out the glucose production assays. L.L. and K.M. carried out the Seahorse experiments together in Prof. Hari Hundal's laboratory. G.R. wrote the manuscript, which was then improved in the light of comments from the other authors. G.R. is the guarantor of this

work and, as such, had full access to all the data in the study and takes responsibility for the integrity of the data and the accuracy of the data analysis.

Parts of this study were presented as a poster abstract to the Diabetes UK Annual Professional Conference, Glasgow, Scotland, 7–9 March 2012.

The authors thank Dr. Benoit Viollet (Université Paris Descartes) and Marc Foretz (Université Paris Descartes) for teaching preparation of mouse primary hepatocytes and assay of glucose production. The authors also thank Prof. Mike Ashford (University of Dundee), Prof. Hari Hundal (University of Dundee), Prof. Steve Keyse (University of Dundee), and Dr. Calum Sutherland (University of Dundee) for helpful discussions and encouragement.

## REFERENCES

1. Slotta KH, Tschesche R. Über Biguanide, II.: Die blutzucker-senkende Wirkung der Biguanide. Ber Dtsch Chem Ges 1929;62:1398–1405
2. Hawgood BJ. Karl Heinrich Slotta (1895–1987) biochemist: snakes, pregnancy and coffee. Toxicon 2001;39:1277–1282
3. Shapiro SL, Parrino VA, Freedman L. Hypoglycemic agents III. N-Alkyl- and arylalkylbiguanides. J Am Chem Soc 1959;81:3728–3736
4. Owen MR, Doran E, Halestrap AP. Evidence that metformin exerts its anti-diabetic effects through inhibition of complex 1 of the mitochondrial respiratory chain. Biochem J 2000;348:607–614
5. El-Mir M-Y, Nogueira V, Fontaine E, Avéret N, Rigoulet M, Leverve X. Dimethylbiguanide inhibits cell respiration via an indirect effect targeted on the respiratory chain complex I. J Biol Chem 2000;275:223–228
6. Hawley SA, Ross FA, Chevtzoff C, et al. Use of cells expressing gamma subunit variants to identify diverse mechanisms of AMPK activation. Cell Metab 2010;11:554–565
7. Kalender A, Selvaraj A, Kim SY, et al. Metformin, independent of AMPK, inhibits mTORC1 in a rag GTPase-dependent manner. Cell Metab 2010;11:390–401
8. Kickstein E, Krauss S, Thornhill P, et al. Biguanide metformin acts on tau phosphorylation via mTOR/protein phosphatase 2A (PP2A) signaling. Proc Natl Acad Sci USA 2010;107:21830–21835
9. Foretz M, Hébrard S, Leclerc J, et al. Metformin inhibits hepatic gluconeogenesis in mice independently of the LKB1/AMPK pathway via a decrease in hepatic energy state. J Clin Invest 2010;120:2355–2369
10. Cameron AR, Anil S, Sutherland E, Harthill J, Rena G. Zinc-dependent effects of small molecules on the insulin-sensitive transcription factor FOXO1a and gluconeogenic genes. Metallomics 2010;2:195–203
11. Zhu M, Lu L, Yang P, Jin X. Bis,(1,1-dimethylbiguanido)copper(II) octahydrate. Acta Crystallogr Sect E 2002;58:m217–m219
12. Ray RK, Kauffman GB. *Metal and Non-Metal Biguanide Complexes*. New Delhi, New Age International Publishers, 1999
13. Ray RK, Kauffman GB. An EPR study of Copper (II)-substituted Biguanide Complexes. Part III. Inorg Chim Acta 1990;174:237–244
14. Ray RK, Kauffman GB. An EPR Study of some copper (II) coordination compounds of substituted biguanides. Part IV. Inorg Chim Acta 1990;174:257–262
15. Rathke B. Ueber Biguanid. Ber Dtsch Chem Ges 1879;12:776–783
16. Slotta KH, Tschesche R. Uber biguanide, I.: Zur Konstitution der Schwermetall-Komplexverbingdungen des Biguanids. Ber Dtsch Chem Ges 1929;62:1390–1398
17. Ray P. Complex compounds of biguanide and guanylureas with metallic elements. Chem Rev 1961;61:313–359
18. Kim BE, Turski ML, Nose Y, Casad M, Rockman HA, Thiele DJ. Cardiac copper deficiency activates a systemic signaling mechanism that communicates with the copper acquisition and storage organs. Cell Metab 2010;11:353–363
19. Logie L, Ruiz-Alcaraz AJ, Keane M, et al. Characterization of a protein kinase B inhibitor in vitro and in insulin-treated liver cells. Diabetes 2007;56:2218–2227
20. Cameron AR, Anton S, Melville L, et al. Black tea polyphenols mimic insulin/insulin-like growth factor-1 signalling to the longevity factor FOXO1a. Aging Cell 2008;7:69–77
21. Rena G, Guo SD, Cichy SC, Unterman TG, Cohen P. Phosphorylation of the transcription factor forkhead family member FKHR by protein kinase B. J Biol Chem 1999;274:17179–17183
22. Rena G, Prescott AR, Guo SD, Cohen P, Unterman TG. Roles of the forkhead in rhabdomyosarcoma (FKHR) phosphorylation sites in regulating 14-3-3 binding, transactivation and nuclear targetting. Biochem J 2001;354:605–612
23. Sakamoto K, Zarrinpashneh E, Budas GR, et al. Deficiency of LKB1 in heart prevents ischemia-mediated activation of AMPKalpha2 but not AMPKalpha1. Am J Physiol Endocrinol Metab 2006;290:E780–E788
24. Wang H-H, Xue L, Fang Z-J, Li G-P, Jiang H. A colorimetric and fluorescent chemosensor for copper ions in aqueous media and its application in living cells. New J Chem 2010;34:1239–1242
25. Sillen LG, Martell AE. Stability constants of metal ion complexes. Chemical Soc London 1971;25(Suppl. 1).
26. Williams RJP. The symbiosis of metal ion and protein chemistry. Pure Appl Chem 1983;55:35–46
27. Sarkar B, Sass-Kortsak A, Clarke R, Laurie SH, Wei P. A comparative study of in vitro and in vivo interaction of D-penicillamine and triethylenetetramine with copper. Proc R Soc Med 1977;70(Suppl. 3):13–18
28. Marongiu G, Lingafelter EC, Paoletti P. Crystal structure of thiocyanatotriethylenetetraminecopper(II) thiocyanate. Inorg Chem 1969;8:2763–2767
29. Fanshawe WJ, Bauer VJ, Ullman EF, Safir SR. Synthesis of unsymmetrically substituted malonamides. J Org Chem 1964;29:308–311
30. Petering HG, Vangiessen GJ. The essential role of cupric ion in the biological activity of 3-ethoxy-2-oxobutyraldehydebisthiosemicarbazone. In *The Biochemistry of Copper*. Peisach J, Aisen P, Blumberg WE, Eds. New York, Academic Press, 1966
31. Ali MA, Mirza AH, Butcher RJ, Rahman M. Nickel (II), copper (II), palladium (II) and platinum(II) complexes of bidentate SN ligands from S-alkyldithiocarbazates and the X-ray structures of the [Ni $(tasbz)_2$] and [Cu$(tasbz)_2$].$CHCl_3$ complexes. Transition Metal Chem 2000;25:430–436
32. Schwarzenbach G, Schwarzenbach D. Complexes of biguanide and malonic-diamidine. J Indian Chem Soc 1977;54:23–24
33. Peisach J, Blumberg WE. A mechanism for the action of penicillamine in the treatment of Wilson's disease. Mol Pharmacol 1969;5:200–209
34. Fryer LGD, Parbu-Patel A, Carling D. The anti-diabetic drugs rosiglitazone and metformin stimulate AMP-activated protein kinase through distinct signaling pathways. J Biol Chem 2002;277:25226–25232
35. Boyle JG, Logan PJ, Ewart MA, et al. Rosiglitazone stimulates nitric oxide synthesis in human aortic endothelial cells via AMP-activated protein kinase. J Biol Chem 2008;283:11210–11217
36. Kassahun K, Pearson PG, Tang W, et al. Studies on the metabolism of troglitazone to reactive intermediates in vitro and in vivo. Evidence for novel biotransformation pathways involving quinone methide formation and thiazolidinedione ring scission. Chem Res Toxicol 2001;14:62–70
37. Sohda T, Mizuno K, Tawada H, Sugiyama Y, Fujita T, Kawamatsu Y. Studies on antidiabetic agents. I. Synthesis of 5-[4-(2-methyl-2-phenylpropoxy)-benzyl]thiazolidine-2,4-dione (AL-321) and related compounds. Chem Pharm Bull (Tokyo) 1982;30:3563–3573
38. Davidoff F. Effects of guanidine derivatives on mitochondrial function. 3. The mechanism of phenethylbiguanide accumulation and its relationship to in vitro respiratory inhibition. J Biol Chem 1971;246:4017–4027
39. Brunmair B, Staniek K, Gras F, et al. Thiazolidinediones, like metformin, inhibit respiratory complex I: a common mechanism contributing to their antidiabetic actions? Diabetes 2004;53:1052–1059
40. Broom WA. The toxicity and glycaemic properties of a number of amidine and guanidine derivatives. J Pharmacol Exp Ther 1936;57:81–97
41. Pryor HJ, Smyth JE, Quinlan PT, Halestrap AP. Evidence that the flux control coefficient of the respiratory chain is high during gluconeogenesis from lactate in hepatocytes from starved rats. Implications for the hormonal control of gluconeogenesis and action of hypoglycaemic agents. Biochem J 1987;247:449–457
42. Campbell MJM, Collis A, Grzeskowiak R. Electron paramagnetic resonance spectrum and covalency parameters of copper-63 (KTS). Bioinorg Chem 1976;6:305–311